1 PPM PRECISION SELF-CALIBRATION OF SCALE FACTOR IN MEMS CORIOLIS VIBRATORY GYROSCOPES

A.A. Trusov[1,2], I.P. Prikhodko[1], D.M. Rozelle[2], A.D. Meyer[2], A.M. Shkel[1]*
[1] MicroSystems Laboratory, University of California, Irvine, CA, USA
[2] Northrop Grumman Electronic Systems – Navigation Systems Division, Woodland Hills, CA, USA

ABSTRACT

We report a scale factor self-calibration in MEMS Coriolis vibratory gyroscopes enabled by real time control of the sense-mode closed loop gain. Similarly to the closed loop scale factor employed in the Hemispherical Resonator Gyroscope (HRG), we measure and remove scale factor changes by injecting a known dither signal (virtual input rate) into the sense-mode dynamics during the normal operation of the gyroscope. The approach was validated using an in-house developed sub-°/hr silicon MEMS Quad Mass Gyroscope (QMG) with HRG-like structural symmetry and low dissipation. We demonstrated a 350 ppm accuracy (limited by the setup) and a 1 ppm precision by simultaneously measuring the true and self-calibrated scale factors over a 10 °C dynamic temperature range.

KEYWORDS

Self-calibration, scale factor, MEMS gyroscope.

INTRODUCTION

Accuracy of MEMS inertial sensors is significantly affected by the drifts in scale factor, limiting their potential application in navigational-grade missions with a 1 ppm stability requirement. Temperature sensitivities on the order of 1000 ppm/°C are a major limiting factor in achieving 1 ppm overall stability in MEMS sensors [1]. Drifts of analog front end gains and other effects contribute to further degradation of scale factor stability. We propose to tackle the issue of scale factor uncertainty by continuous self-calibration of the gyroscope sense-mode gain during its normal operation. In contrast to periodic offline physical re-calibration of rate sensors using sophisticated inertial characterization equipment, the new approach eliminates the need for a high accuracy absolute rotation reference or any other physical stimulus.

Similarly to the Closed Loop Scale Factor (CLSF) [2] approach employed in the macro-scale fused quartz navigational-grade Hemispherical Resonator Gyroscope (HRG), the method relies on a virtual input rate injection to continuously observe and compensate drifts. Although a gyroscope is operated in force-to-rebalance (FTR)-mode of operation, the key factor enabling 1 ppm scale factor self-calibration is the whole-angle (WA)-mode, which provides a stable in-situ reference (angular gain is long-term stable down to ppb). An in-house developed sub-°/hr silicon MEMS Quadruple Mass Gyroscope (QMG) [3,4] capable of both WA [5] and FTR-modes of operation was chosen for the approach validation due to its HRG-like structural parameters (operational anti-phase frequency of 2 to 3 kHz, measured Q-factors above 1 million, complete frequency and damping symmetry).

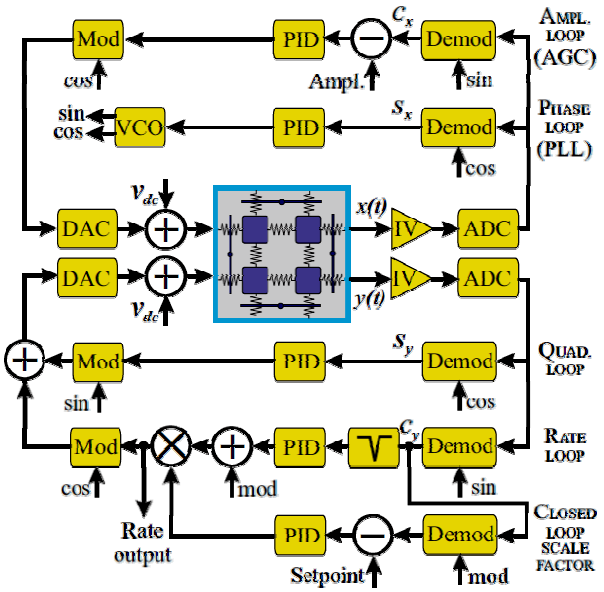

Figure 1: QMG control loops: force-to-rebalance (FTR) and closed loop scale factor (CLSF). Virtual input rate is injected to observe and correct for scale factor drifts.

FORCE-TO-REBALANCE ANALYSIS

This section reviews FTR rate gyroscope operation to provide framework for the CLSF self-calibration.

Principle of Operation

FTR operation [6] is used to improve the bandwidth of-mode-matched high-Q gyroscopes while taking advantage of their inherently high sensitivity and low noise. As shown in Fig. 1, the gyroscope's drive-mode is operated at mechanical resonance ω_x using a Phase-Locked Loop (PLL). The amplitude of drive-mode motion is stabilized by an Automatic Gain Control (AGC). The sense-mode amplitude is maintained at zero by applying a rebalancing force which includes the Coriolis and quadrature signals. This allows increasing the bandwidth of the mode-matched gyroscope using feedback control of the sense-mode.

The rate (FTR) and quadrature loops operate similarly to the drive-mode amplitude control loop, but with a zero set point. The ratio of the sense-mode Coriolis channel rebalancing force f_y to the drive-mode amplitude control force f_x is used to measure the input rate [6]:

$$f_y / f_x = Q_x \left(2k\Omega_z + \Delta(1/\tau)\sin 2\theta_\tau\right)/\omega_x , \qquad (1)$$

where Q_x is the drive-mode Q-factor, k is the angular gain factor, $\Delta(1/\tau)$ is the decay time constant mismatch between drive- and sense-modes, and θ_τ is the angle of the principal axis of damping. Eq. (1) highlights that the damping mismatch $\Delta(1/\tau)$ is a major source of drift in the gyroscope.

Bandwidth

Bandwidth of the FTR rate loop is a critical parameter since it must not interfere with the operation of the CLSF dither signal. Otherwise, the frequency domain based separation of the true inertial input from the virtual input (dither signal) introduced by the CLSF calibration loop is impossible. The bandwidth analysis assumes the gyroscope dynamics is governed by:

$$\ddot{y} + (\omega_y / Q_y)\dot{y} + \omega_y^2 y = f_y - (2k\Omega_z + \Delta(1/\tau)\sin 2\theta_\tau)\dot{x}, \quad (2)$$

where y, ω_y and Q_y are the sense-mode displacement, frequency and Q-factor, respectively. Here, the drive-mode motion x is controlled by AGC and PLL loops to sustain an oscillation with a stable amplitude a_0, $x = a_0 \cos\omega_x t$.

FTR control laws are formulated in terms of the in-phase c_y and quadrature s_y components of the y signal:

$$y = c_y \cos(\omega t + \phi) + s_y \sin(\omega t + \phi), \quad (3)$$

where $\cos(\omega t + \phi)$ and $\sin(\omega t + \phi)$ are the reference signals generated by PLL operating at the frequency $\omega = \omega_x + \dot{\phi}$. The c_y component proportional to the input rate is always rebalanced (zeroed) by the proportional-integral (PI) controller with the gain K_{cy} and integral time τ_{cy} [7]:

$$f_y = K_{cy}\left[c_y + (1/2\tau_{cy})\int_0^t c_y(\tau)d\tau\right]\sin(\omega t + \phi). \quad (4)$$

Substituting (3) and (4) into (2), we obtain equation

$$\dot{c}_y + 2c_y/\tau_\Omega + \omega_\Omega^2 \int_0^t c_y d\tau = -(2k\Omega_z + \Delta(1/\tau)\sin 2\theta_\tau)a_0/2, \quad (5)$$

which can be used to analyze the transient response and bandwidth [7]. Here $\tau_\Omega = 4\omega/K_{cy}$ and $\omega_\Omega = K_{cy}/(4\omega\tau_{cy})$ are the values of settling time and the rate-loop bandwidth.

Similarly to Eq. (2), the derivative of Eq. (5) is an equation of damped, linear, second order system with bandwidth ω_Ω and settling time τ_Ω defined by controller's proportional (P) and integral (I) gains K_{cy} and K_{cy}/τ_{cy}. In contrast to the open-loop operation, the closed-loop FTR bandwidth and settling time can be adjusted without sacrificing the low noise of the sense-mode. This is critical for high-Q rate sensors since the-mode-matching in open loop operation limits their measurement bandwidth. The open-loop settling time is given by the energy decay time constant $\tau = 2Q_y/\omega$, which for Q values greater than 1 million and frequencies below few kHz reaches several minutes, making it practically impossible to measure fast changes of the input rotation. The closed loop FTR operation resolves the gain-bandwidth tradeoff while preserving low noise operation of high-Q devices.

CLOSED LOOP SCALE FACTOR

This section presents adaptation of the CLSF approach [2] to mode-matched high-Q MEMS gyroscopes

Principle of Operation

Fig. 1 shows FTR and CLSF control loops, which continuously observe and adjust the sense-mode gain (scale factor). CLSF relies on adding a square-wave modulation signal to the FTR command (feedback signal, f_y) and observing the output angle precession of the gyroscope. The self-calibration closed-loop is added to the four existing loops without interrupting the gyroscope normal FTR operation. This is possible because the frequency of the modulation signal is chosen to be outside of the gyroscope bandwidth. It also allows separating the inertial input information from the modulated signal in frequency domain.

The injected modulation signal acts as a virtual input rate $\Omega_{r\text{-mod}}$ and deviates the vibration pattern angle of the gyroscope from its nominal null position through the use of WA-mode. By comparing the angle output relative to the integrated virtual input, the scale factor change is made observable. The scale factor estimate is fed to the PI controller to form the CLSF feedback command. A notch filter is employed to remove the self-calibration dither signal from the sensor output. This way the CLSF loop does not interfere with the FTR operation. To perform an active self-calibration, the CLSF feedback signal is used to continuously regulate the loop gain by changing the forcer gain K_{fy}.

Dynamics

Dynamics of a FTR gyroscope operated with CLSF can be described as:

$$\ddot{y} + (\omega_y/Q_y)\dot{y} + \omega_y^2 y = (K_{fy} f_y - 2k\Omega_z)\dot{x} + \Omega_{r-\text{mod}}\dot{x}, \quad (6)$$

with two inputs (true rate Ω_z and virtual rate $\Omega_{r\text{-mod}}$). Here, the $\Delta(1/\tau)$ term is omitted for clarity. The c_y component of the gyroscope output contains responses to both inputs, which are separated by using a notch filter. While the filtered c_y component is used in the FTR rate-loop controller to rebalance the term $(K_{cy}f_y - 2k\Omega_z)$ to zero, the raw c_y signal is used to form the scale-factor error estimate for the CLSF controller and adjust its gain K_{cy}.

When FTR loops are in place, the dynamics simplifies to:

$$\ddot{y} + (\omega_y/Q_y)\dot{y} + \omega_y^2 y = \Omega_{r-\text{mod}}\dot{x}, \quad (7)$$

and the steady-state solution in terms of c_y is given by [6]:

$$c_y = a_0 \int_0^\tau \Omega_{r-\text{mod}}(\tau)d\tau = a_0\Theta_{r-\text{mod}}. \quad (8)$$

which is the WA output. Eq. (8) shows that for ideal case, the measured output angle Θ is exactly the integral of the virtual input rate $\Theta_{r\text{-mod}}$. In reality, however, errors such as analog front-end gain drift lead to the output change. The angle difference is used to observe the scale factor error:

$$c_y - a_0 \int_0^\tau \Omega_{r-\text{mod}}(\tau)d\tau = a_0(\Theta - \Theta_{r-\text{mod}}). \quad (9)$$

Alternatively, scale factor change can be observed by demodulating the raw c_y output with the $\Theta_{r\text{-mod}}$ reference input. This approach is implemented in the current paper.

EXPERIMENTAL RESULTS

This section experimentally validates the CLSF self-calibration using the Quadruple Mass Gyroscope (QMG).

Sensor and Electronics

To investigate the feasibility of CLSF for MEMS, we performed a series of experiments using a first generation silicon MEMS QMG [3] with natural frequencies of 2.2 kHz and measured Q-factors of 1.2 million with $\Delta Q/Q$ of ±1%. This gyroscope previously demonstrated an angle random walk (ARW) of 0.02 °/√hr and in-run bias instability of 0.2 °/hr [4]. The vacuum packaged QMG was mounted on a PCB with front-end electronics and mounted on a 1291 Ideal Aerosmith precision rate table equipped with a thermally controlled chamber.

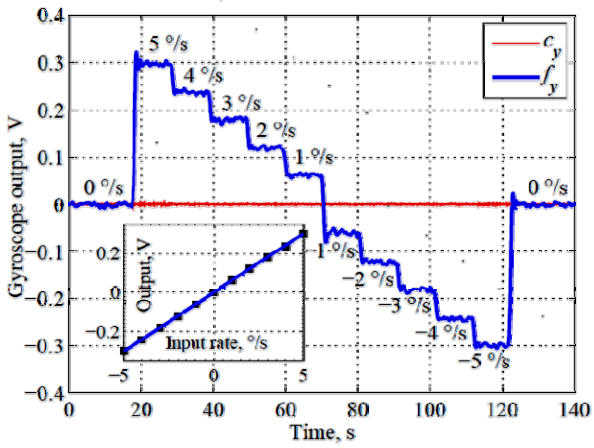

Figure 2: Rate response in 5 °/s range, showing 0.5% RMS linearity and no interference of CLSF and FTR loops.

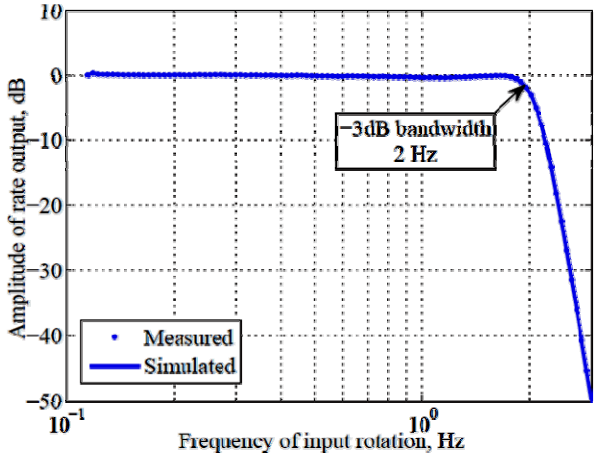

Figure 3: FTR rate-loop bandwidth measured to be 2 Hz by applying sinusoidal rotation with different frequencies.

Electrostatic actuation and capacitive detection were employed along with the EAM technique for the parasitic feed-through elimination. All control and signal processing were realized using a LabView programmable HF2LI Zurich Instruments unit and a high-stability SRS DS345 signal generator square-wave modulation.

Force-to-Rebalance Characterization

Fig. 2 shows the measured response to input rotation rates in a ±5°/s range using an FTR instrumented QMG. The data confirms that the sense-mode signal c_y remained zero in presence of applied rotations, while the force required to rebalance the motion f_y was proportional to the applied rate with a 0.5% full scale RMS linearity. A wide full scale rate range of 150 °/s was achieved despite the ultra-high Q-factor and was only limited by the maximum available forcer voltage of 10 V.

For the proof of concept demonstration of the self-calibration, the PI gains in Eq. (5) were chosen to set a 2 Hz FTR loop bandwidth, while the modulation signal for the CLSF loop was set at 7 Hz. The bandwidths of AGC, PLL and quadrature loops was set to be 0.5 Hz, 15 Hz, and 2 Hz, respectively. Despite the QMG ring down time constant of 172 s and a fast 300 °/s^2 rate table acceleration, the measured settling time of 0.5 s (Fig. 2) was in a good agreement with the 2 Hz FTR rate-loop

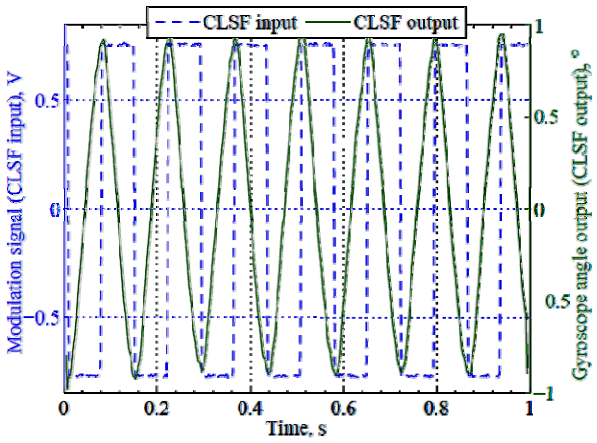

Figure 4: Measured input and output signals of the CLSF self-calibration loop used to estimate scale factor change.

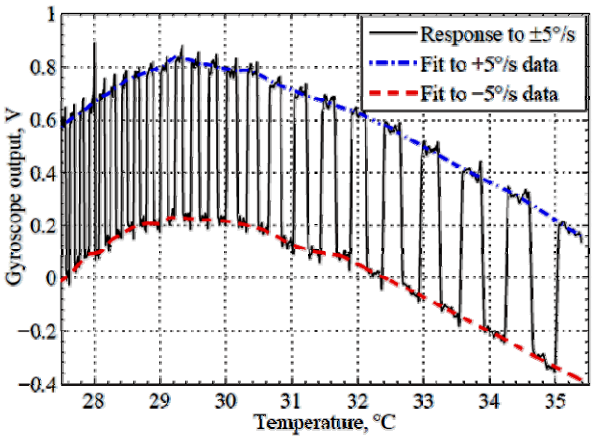

Figure 5: QMG rate output in response to physical ±5 °/s input rotations, used to characterize the true scale factor.

bandwidth, Fig. 3. Further characterization revealed that rate noise performance of FTR-operated gyroscope can approach that of the open-loop high-Q sensor.

Closed Loop Scale Factor Characterization

While the nominal scale factor of 0.06 (°/s)/V was initially obtained using the rate table (Fig. 2), its relative change or drift was observed in real-time by amplitude demodulation of the QMG angle output (CLSF output) at frequency of the injected modulation signal (CLSF input), Fig. 4. The square-wave modulation signal acts as a virtual rate input, and according to Eq. (8) the WA output of the gyroscope is equal to the integral of this signal, which is the triangular wave signal.

To analyze CLSF accuracy, a true scale factor of the QMG was continuously observed by applying constant ±5 °/s physical rotations while changing temperature from 25 °C to 35 °C, Fig. 5. At the same time, the CLSF provided an estimate of scale factor drift. Fig. 6(a) shows an experimental comparison of the true and estimated scale factor change over the 10 °C dynamic temperature range, demonstrating a close match between values. The RMS accuracy (difference between the true and estimated values) was measured to be 350 ppm, Fig. 6(b), confirming that CLSF output can be used to observe and correct the gyroscope's true scale factor drift. The

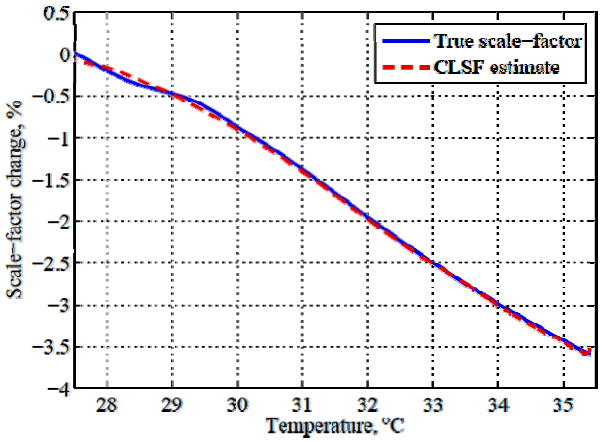

(a) A close match between the measured true scale factor and CLSF estimate demonstrates feasibility of the scheme.

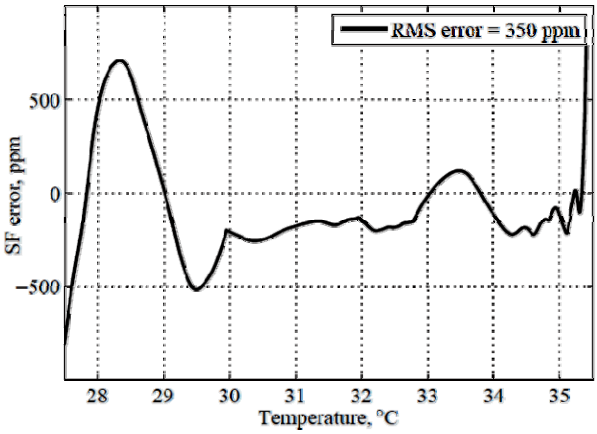

(b) Demonstration of a 350 ppm CLSF accuracy obtained by subtracting estimated CLSF from the true scale factor.

Figure 6: Experimental comparison of the true and CLSF errors over a 10 °C dynamic temperature range.

accuracy of the experiment was limited by the 100 ppm (0.01 %) rate table accuracy specified by the datasheet.

To perform an active self-calibration, the CLSF feedback command was used to continuously regulate the loop gain of the QMG using a PI controller, yielding a stable scale factor. Allan deviation analysis of the closed loop scale factor showed that 30 ppm precision is achieved after 1 minute of self-calibration, Fig. 7. Upon 30 minutes of operation, 1 ppm precision is achieved, demonstrating potential of MEMS gyroscope self-calibration for inertial-grade performance.

CONCLUSIONS

Scale-factor self-calibration was implemented using an in-house developed sub-°/hr Quadr Mass Gyroscope capable of both whole angle and force-to-rebalance-modes of operation. The self-calibration works since the injected modulation signal (virtual rate) passes through the gyroscope dynamics and analog front-end electronics in the same manner as does the true inertial input rate signal. We demonstrated 350 ppm accuracy by simultaneously measuring the true and self-calibrated scale factors over 10 °C dynamic temperature range. The precision of self-calibration was 1 ppm after 2000 s of averaging. The ongoing work on rate table encoder

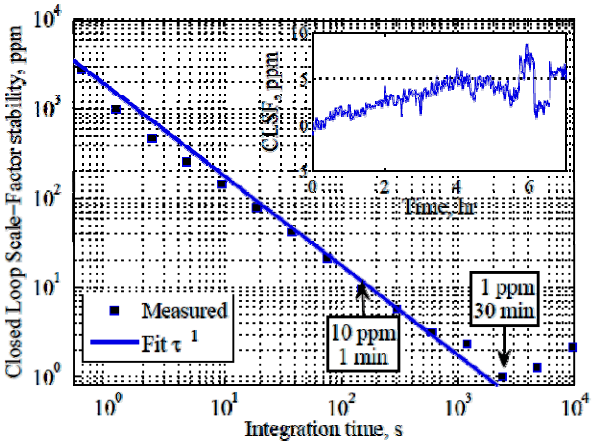

Figure 7: Allan deviation analysis shows that 1 ppm precision of CLSF is achieved upon 2000 s of averaging.

synchronization is deemed to result in demonstration of better than 100 ppm scale-factor self-calibration accuracy. We believe that our initial results demonstrate an intriguing new approach to the next level improvement in inertial MEMS performance and motivate future research and development of self-calibration techniques.

ACKNOWLEDGEMENTS

This work was supported by the DARPA/SPAWAR under Contract N66001-12-C-4035, program manager Dr. William Chappell. The devices were designed and tested at the MicroSystems Laboratory, UC Irvine.

REFERENCES

[1] M.S. Weinberg, A. Kourepenis, "Error sources in in-plane silicon tuning-fork MEMS gyroscopes," *J. Microelectromech. Syst.*, vol. 15, no. 3, pp. 479–491, 2006.

[2] D.M. Rozelle, "Closed loop scale factor estimation," *US patent 7,628,069*, Dec. 8, 2009.

[3] A.A. Trusov, A.R. Schofield, A.M. Shkel, "Micromachined tuning fork gyroscopes with ultra-high sensitivity and shock rejection," *US Patent 8,322,213*, Dec. 4, 2012.

[4] I.P. Prikhodko, S.A. Zotov, A.A. Trusov, A.M. Shkel, "Sub-degree-per-hour silicon MEMS rate sensor with 1 million Q-factor," in *Digest Tech. Papers Transducers'11 Conference*, Beijing, China, June 5–9, 2011, pp. 2809–2812.

[5] I.P. Prikhodko, S.A. Zotov, A.A. Trusov, A.M. Shkel, "Foucault pendulum on a chip: rate integrating silicon MEMS gyroscope," Sensors and Actuators A: Physical, Vol. 177, pp. 67–78, April 2012.

[6] D. Lynch, "Coriolis vibratory gyros," in: Symposium Gyro Technology 1998, pp. 1.0–1.14. (Reproduced as Annex B, Coriolis Vibratory Gyros, pp. 56–66 of IEEE Std. 1431-2004).

[7] D. Lynch, "Vibratory gyro analysis by the method of averaging," Proc. 2nd St. Petersburg Int. Conf. on Gyroscopic Technology and Navigation, pp. 26–34. 1995.

CONTACT

*A.A. Trusov, alex.trusov@gmail.com